Journal of Ginseng Research 46 (2022) 464–472

Contents lists available at ScienceDirect

Journal of Ginseng Research

journal homepage: https://www.sciencedirect.com/journal/journal-of-ginseng-research

Research Article

Effect of Lactobacillus dominance modified by Korean Red Ginseng on the improvement of Alzheimer's disease in mice

Mijung Lee [a], So-Hee Lee [a], Min-Soo Kim [b], Kwang-Sung Ahn [b], Manho Kim [a, c, d, *]

[a] Department of Neurology, Biomedical Research Institute, Seoul National University Hospital, Seoul, Republic of Korea
[b] Functional Genome Institute, PDXen. Biosystem Co., Gyeongi-do, Republic of Korea
[c] Neuroscience Dementia Research Institute, Seoul National University College of Medicine, Seoul, Republic of Korea
[d] Protein Metabolism Medical Research Center, College of Medicine, Seoul National University Hospital, Seoul, Republic of Korea

ARTICLE INFO

Article history:
Received 9 May 2021
Received in revised form
8 October 2021
Accepted 4 November 2021
Available online 11 November 2021

Keywords:
Lactobacillus
Korean Red Ginseng
Gut-brain axis
Alzheimer's disease

ABSTRACT

Background: Gut microbiota influence the central nervous system through gut-brain-axis. They also affect the neurological disorders. Gut microbiota differs in patients with Alzheimer's disease (AD), as a potential factor that leads to progression of AD. Oral intake of Korean Red Ginseng (KRG) improves the cognitive functions. Therefore, it can be proposed that KRG affect the microbiota on the gut-brain-axis to the brain.

Methods: Tg2576 were used for the experimental model of AD. They were divided into four groups: wild type (n = 6), AD mice (n = 6), AD mice with 30 mg/kg/day (n = 6) or 100 mg/kg/day (n = 6) of KRG. Following two weeks, changes in gut microbiota were analyzed by Illumina HiSeq4000 platform 16S gene sequencing. Microglial activation were evaluated by quantitative Western blot analyses of Iba-1 protein. Claudin-5, occludin, laminin and CD13 assay were conducted for Blood-brain barrier (BBB) integrity. Amyloid beta (Aβ) accumulation demonstrated through Aβ 42/40 ratio was accessed by ELISA, and cognition were monitored by Novel object location test.

Results: KRG improved the cognitive behavior of mice (30 mg/kg/day $p < 0.05$; 100 mg/kg/day $p < 0.01$), and decreased Aβ 42/40 ratio ($p < 0.01$) indicating reduced Aβ accumulation. Increased Iba-1 ($p < 0.001$) for reduced microglial activation, and upregulation of Claudin-5 ($p < 0.05$) for decreased BBB permeability were shown. In particular, diversity of gut microbiota was altered (30 mg/kg/day q-value<0.05), showing increased population of Lactobacillus species. (30 mg/kg/day 411%; 100 mg/kg/day 1040%).

Conclusions: KRG administration showed the Lactobacillus dominance in the gut microbiota. Improvement of AD pathology by KRG can be medicated through gut-brain axis in mice model of AD.

1. Introduction

Alzheimer's disease (AD) is one of the most serious neurodegenerative disease that affects the elderly [1]. Non-cognitive behavioral problems and cognitive impairments, such as memory, language, spatial perception, or other cortical dysfunction, progress as major signs of dementia [2]. The mechanisms of the disease have been elucidated to some extent through experimental studies on the brain at the molecular and cellular level [3]. Although hundreds of clinical trials have been made, there are currently no available pharmacological therapies to completely prevent the progression of disease [4,5]. Amyloid beta (Aβ) aggregation and its signaling cascades have been proposed as the major cause for neurotoxicity along with microglia activation [6–10]. Phosphorylated tau or oligomers are increasingly reported as another major factor in the development of AD pathogenesis. Altered gut microbiota in healthy individuals has been reported to be associated with several disorders such as Parkinson's disease [11], schizophrenia [12], type 1 diabetes mellitus [13,14], hypertension [15,16], or Behcet's disease [17]. Furthermore, disruption of gut microbiota environment also plays a role in the development of AD-related pathogenesis [18].

Metabolites such as short chain fatty acids (acetate, butyrate, and propionate) from gut microbiota dysregulation results in an increase of blood brain barrier (BBB) permeability, so that the

Abbreviations: AD, (Alzheimer's disease); BBB, (Blood-brain barrier); KRG, (Korean Red Ginseng); Aβ, (Amyloid beta); ELISA, (enzyme-linked immunoassay).

* Corresponding author. Department of Neurology, Seoul National University Hospital, 101 Daehak-ro, Jongno-gu, Seoul, 03080, Republic of Korea.
E-mail address: kimmanho@snu.ac.kr (M. Kim).

https://doi.org/10.1016/j.jgr.2021.11.001

metabolites can pass through the BBB [11,19]. Thus, the gut microbiota affects the development of synapses, control of neurotransmitters, or release of neurotrophic factors in the brain [20,21]. Therefore, restoring the altered gut microbiota can be one of the strategies for modulating AD.

Korean Red Ginseng (KRG) has shown pleiotropic effects on memory deterioration, inflammation, cancer, or cardiovascular disease without severe side effects [2,6,22,23]. Effects of KRG on AD have been described as neuroprotective point of view within the brain [24–30]. Further exploration for the ingested KRG on AD is required from the gut microbiota perspective.

Here, we replicated the effect of KRG on improving AD in the transgenic mice model of AD. Behavioral performance, BBB permeability, Aβ accumulation, and microglial activation were analyzed in accordance with the changes in the microbiota, to demonstrate the potential of modulating AD by KRG through gut-brain axis.

2. Materials and methods

2.1. Animals and experimental groups

Institutional Animal Care and Use Committee of Seoul National University Hospital (IACUC, Approval number: 19-0126-S1A1) approved all procedures for animal experiment performed in this work. IACUC was certified by the Association for the Assessment and Accreditation of Laboratory Animal Care International. Tg2576 heterozygous transgenic mice expressing the human APP (from Dr. Inhee Mook-Jung, Seoul National University Hospital) were used. Solid feeds and filtration-purified water for laboratory animal are freely offered. The mice were housed in groups having a 12 h light/12 h dark cycle, and food and water are accessed to ad libitum. Nine-month-old male Tg2576 mice were randomly assigned to four groups: 1.WT (n = 6), 2. Tg2576 (n = 6), 3. KRG 30 mg/kg/day group (n = 6), and 4. KRG 100 mg/kg/day group (n = 6).

2.2. KRG administration

Korea Ginseng Corporation (Daejeon, Korea) provided the KRG extract used in this work. In short, steaming of ginseng was performed at 90–100 °C for 3 h without additional pressure followed by drying at 50–80 °C, and extracted three times for 8 h each with circulation of hot water of 85–90 °C. Then the extract was diluted with sterilized water. The pooled extract contained water equivalent to 36% of the total weight. The ginsenoside compositions of crude extract were analyzed through HPLC by Kim et al. [31].

The number of mice in each group were set to 4 males. The dosage was set so as not to exceed 0.02 ml/g. The body weight that was used in calculation was measured immediately before the administration. Test substances were mixed well with sterile distilled water. They are administered by oral using sonde every day for two weeks. The material used as the reference material is sterile distilled water.

2.3. Monitoring of behavior and lethality

For 6 h after oral administration, starting from the next day, not only the onset of addiction but also changes in the overall condition were observed. Abnormal behavior that could be expressed by test substances were carefully observed. The type and severity of symptoms were individually recorded in the case of abnormality. The death or critical condition of all mice has been identified.

2.4. Measurement of weight

Changes in body weight were measured for all animals immediately prior to administration of the test substance twice a week at a specific time for two weeks.

2.5. Novel object location testing

We used pre-tests of new object location operations that depend on the hippocampus to ensure similar native memory performance between groups. After a one-week acclimation period, mice were treated daily for three days. Mice were transferred from home cage to a testing cage and acclimated for 30 min on the fourth day for training the new object. Testing cage is an open chamber made of acrylic glass (50 × 50 × 50 cm), and mice were placed in the chamber for 5 min. Two different objects were placed in the chamber and three trials of 5 min were given to mice for exploring objects with interval of an hour between each trial. Mice were returned from the testing cage to their home cages between each trial. After 24 h from training, the mice were again transferred from home cage to a testing cage with 30 min of acclimation time, and the same two objects used for the training of the previous day were brought. The two objects were placed in two different locations with the same distance from the wall of the chamber. The mice were allowed to explore these objects in the chamber for 5 min. Mice were again returned from the testing cage to their colony room after the test.

We cleaned the chamber and objects between each trial with ethanol to reduce odor cues. The objects were fixed with double-sided tape on the bottom of the chamber so that the objects could not be moved by the mice. Behaviors were recorded. The time spent by mice in the center of the chamber (70% of the total area) and travel speed were quantified by TOPSCSn. Investigation status of mice for an object was defined as a nose pointed to an object with distance less than one centi-meter. .

2.6. Collection of feces

Fresh feces from mice were collected by sterilized EP tubes, followed by quick freezing using dry ice, and they were moved into a −80 °C cryogenic freezer for storage before DNA extraction.

2.7. DNA extraction and 16S rRNA gene amplification sequence processing

Samples were centrifuged at 15 K rpm for 30 min at 4 °C to separate the cellular pellet from cell-free supernatant. DNAs were extracted from the pellet by a QIAamp DNA Microbiome Kit (Qiagen, Valencia, CA, USA) according to manufacturer's instructions.

The amplification of the 16S rRNA gene in the V3–V4 region was conducted using the 341F (5′ TCG TCG GCA GCG TCA GAT GTG TAT AAG AGA CAG CCT ACG GGN GGC WGC AG 3′) and 805R (5′ GTC TCG TGG GCT CGG AGA TGT GTA TAA GAG ACA GGA CTA CHV GGG TAT CTA ATC C 3′) primers. Illumina adaptor overhang sequences were also added. Amplicon has been purified with a cleaning system based on magnetic beads. (Agencourt AMPure XP; Beckman Coulter, Brea, CA, USA). Libraries were indexed by Nextra technology using limited cycle PCR followed by further cleaning, and pooled to the same molar concentrations. The final library was denatured by 0.2 N NaOH followed by dilution using a 20% PhiX control to 6 pM. We performed the sequencing using a 2 × 300 bp paired-end protocol on Illumina MiSeq platform, following the manuals.

2.8. Metagenomic analysis

From 24 fecal samples, total genomic DNA was extracted using the E.Z.N.A. Stool DNA kit (Omega Bio-Tek, USA) according to the manuals. Fragments of DNA having average size of approximately 300 bp were prepared by using TruSeq DNA Sample Prep Kit. Paired-end library was constructed by Covaris M220 (Gene Company Limited, China). Using Illumina HiSeq4000 sequencing platform (Illumina Inc., San Diego, CA, USA), the metagenomic sequencing was performed following the manuals. The raw data of sequence reads were truncated to less than quality scores of 20 points and shorter than 50 bp in length. Then the SOAPdenovo software was used to assemble the clean raw reads to get the contigs for the next predictions. MetaGene (http://metagene.nig.ac.jp) was used to predict the ORFs (Open reading frames) from each sample. The annotation of COG (cluster of orthologous groups of proteins) from the ORFs were analyzed by using the BLASTP (BLAST Version 2.2.28+) in eggNOG database (Version 4.5) with a cutoff value of 10^{-5}.

2.9. Bioinformatics and statistic analysis

The primary analysis on the obtained sequences with demultiplexation was performed by the Illumina MiSeqReporter software. For analysis in FASTA format, the paired-end sequence of each sample was exported from the MiSeq system. The bioinformatic analysis was performed with the QIIME2 package for the sequences [32]. Microbiome Analyst [33] was used for subsequent data analysis. Sequences were clustered against the 97% reference data set of the 2013 Green genes (13_5 release) ribosomal database [34]. Sequences that did not match any entries in this reference were clustered into de novo OTUs (operational taxonomic units) at 97% similarity using UCLUST. For further analysis, the OTU table was diminished to a sequencing depth of 20 K per sample.

Taxonomic analyses were performed after collapsing OTUs at the genus level. Shannon index was used to evaluate the alpha diversity of each sample. Bray-Curtis exponential distance method was used to determine beta diversity, and PCoA (principal coordinate analysis) plots were created. The statistical significance was evaluated by non-parametric uni-variable Mann-Whitney/Kruskal-Wallis test for different sampling sites and gut regions of mice gut microbiota. Identification of difference in abundances of bacterial taxa were performed by Linear discriminant analysis effect size (LEfSe). The false discovery rate (FDR) correction was accessed for multiple tests. P value less than 0.05 was considered statistically significant.

Linear discriminant analysis (LDA) and linear discriminant analysis effect Size (LEfSe) were used to determine the statistically significant differences in the relative abundance of genera between strains of mice. Criteria that are considered statistically significant are those with an LDA value greater than 2.5 at a P value less than 0.05. LDA and LEfSe were used for metagenomic analysis to identify what differed significantly in the COG and KEGG categories between mouse strains. Criteria that are considered statistically significant are those with an LDA value greater than 2.5 at a P value less than 0.05.

2.10. Tissue preparation and fluorescent immunohistochemistry

For immunohistochemistry, cold saline of 10 ml and paraformaldehyde of 4% in 0.1 M PBS were used to anesthetize mice by perfusing through the heart. Then we harvested the brain quickly, and post-fixed in PFA of 4% for 48 h, and immersed in sucrose solution of 30%. They were storaged at 4 °C prior to be sectioned. Frozen sections were then cut by a thickness of 10 μm. Sections floating freely were washed by phosphate-buffered saline and blocked with Triton X-100 of 0.3% and normal blocking serum in PBS (10%) for 1 h at room temperature. Then they were stained overnight at 4 °C using the Claudin-5 (1:50; Santa Cruz Biotechnology, Santa Cruz, CA, USA), Occludin (1:50; Santa Cruz Biotechnology, Santa Cruz, CA, USA), CD13(1:50; Abcam, Cambridge, United Kingdom), Laminin (1:100; Santa Cruz Biotechnology, Santa Cruz, CA, USA) and β-amyloid (1:50; Santa Cruz Biotechnology, Santa Cruz, CA, USA) primary antibody. The next day, PBS was used to wash sections and sections were incubated for 2 h with Cy3 conjugated anti-mouse IgG and Cy3 conjugated anti-rabbit IgG (1:100; Jackson immune Research Laboratories). Cells were stained by Occludin, Claudin-5, CD13, Laminin (red) or DAPI (blue). They were analyzed through an upright microscope (Ni-E, Nikon Corporation, Tokyo, Japan).

2.11. Quantification of Aβ 1–40 and Aβ 1-42

Sandwiched Aβ ELISA was accessed to evaluate the whole brain levels of Aβ 1–40 and Aβ 1–42 in six animals of each experimental groups. Supernatant fractions were accessed by Aβ 1–40 and Aβ 1–42 ELISA kits (KMB 3481 and KMB 3441, respectively; Invitrogen, Camarillo, CA, USA) which is pre-established for mouse to quantify Aβ levels, following the manuals.

Monoclonal antibody has been coated onto microplates, which is specific for mouse Aβ 1–40 or Aβ 1–42. To the center of each well, we added standard or samples of 50 μl, then added buffer of 50 ml for assay dilution. Room temperature incubation for 3 h, and five times of washing were treated to each well. Then mouse Aβ 1–40 or Aβ 1–42 conjugate of 100 ml was added to wells and incubated for additional 1 h followed by repeated cleaning. Finally, wells were incubated for 30 min in substrate solution of 100 ml, and the stop solution was used to stop the reaction. The analyses were always done with multiple duplicates. Values of OD450 were detected by a microplate reader (Multiskan EX; Thermo Electron Corporation, Vantaa, Finland). Calculation of the Aβ 1–40 and Aβ 1–42 levels were done by following the standard curve.

2.12. Western blot analysis and extraction of protein

Brain of Tg2576 mice was isolated followed by quick freezing by liquid nitrogen, and it was moved into a −80 °C cryogenic freezer for storage before the extraction of proteins. RIPA buffer (Radio immunoprecipitation assay buffer, Thermo-Scientific, Waltham, MA, USA) with protease inhibitor and phosphatase inhibitor (Roche, NJ, USA) in fresh condition was used to perform protein extraction. BCA (Bicinchoninic acid assay) protein assay kit (Pierce, Rockford, IL, USA) was used to identify the protein content. Separation of 40 μg of protein samples were conducted through sodium dodecyl sulfate-polyacrylamide gel electrophoresis (SDS-PAGE, 4–15% Novex NuPage Bis-Tris gel, Invitrogen, Mount Waverley, Australia) followed by transfer onto polyvinylidene fluoride membrane (PVDF, Millipore, Bedford, MA, USA). Then, 5% non-fat dried milk dissolved in 1 × TBST (Tris-buffered saline with 0.1% v/v Tween-20) was treated on them at room temperature for an hour. Incubation during overnight at 4 °C with the diluted primary antibodies was done on the blots, following the manuals. Occludin (1:200; Santa Cruz Biotechnology, Santa Cruz, CA, USA), Claudin-5 (1:200; Santa Cruz Biotechnology, Santa Cruz, CA, USA), Iba1 (1:200; Santa Cruz Biotechnology, Santa Cruz, CA, USA) and anti-β-actin (1:200, Santa Cruz Biotechnology, Santa Cruz, CA, USA) were used as the primary antibody. Further incubation for blots were conducted with anti-rabbit antibodies (1:3000, GE Healthcare, NJ, USA) or horseradish peroxidase-conjugated secondary anti-mouse. Blots were then developed by ECL solution (Enhanced

chemiluminescenece solution, Advansta, CA, USA). Three independent results normalized by β-actin were used for the evaluation of band intensities in Image J software. All data are displaying the representative ones from three independent experiments.

2.13. Statistical analysis

All values indicated in the figures are presented as mean ± standard deviation. Neuman-Keuls post hoc test for one-way analysis of variance was used to compare those groups. Prism 5 software (GraphPad Software Inc., La Jollla, CA, USA) was used for all statistical tests. Criteria that are considered statistically significant are those with a P value less than 0.05.

3. Results

3.1. Improvement of the cognitive function by KRG

We compared four experimental groups to analyze the effect of KRG in the mice model of AD: 1. WT (wild type), 2. Tg2576-Control (transgenic AD mice without KRG treatment, 3. Tg2576-ST(Full name) 30 mg/kg/day, and 4.Tg2576-ST 100 mg/kg/day (transgenic AD mice with KRG treatment by a given dosage of 30 mg/kg/day and 100 mg/kg/day, respectively).

The novel object recognition test was used for measuring memory (Fig. 1A). Tg2576-Control group had less tendency for recognizing novel objects compared to that of WT group. KRG-administrated group presented a significant increase of exploration compared to non-treated transgenic mice, thus indicating the enhanced memory (30 mg/kg/day $p < 0.05$; 100 mg/kg/day $p < 0.01$; Fig. 1B).

3.2. Reduction of Aβ accumulation by KRG ingestion

Improvement of AD pathology through the reduction of Aβ accumulation by KRG intake was confirmed by ELISA. Tg2576-Control group had higher level of Aβ accumulation than that of WT group. KRG treatment decreased Aβ 42/40 ratio (Tg2576-ST 30 mg/kg/day $p < 0.01$; Tg2576-ST 100 mg/kg/day $p < 0.01$; Fig. 2A). Immunofluorescence staining showed the Aβ accumulation in Tg2576-Control group, but not in WT group. Unlike the results of ELISA, the change in Aβ accumulation was not discriminated by KRG in this experiment (Fig. 2B).

3.3. Reduction of microglial activation

Aβ accumulation occurs along with microglial activation that lead to neuronal death, resulting the progression of AD. Quantitative Western blot analysis showed that Iba-1, a marker for activated microglia, increased in Tg2576 when compared to WT ($p < 0.001$) (Fig. 3). Furthermore in Tg2576-ST 30 mg/kg/day group, Iba-1 protein levels were comparable to that of WT.

3.4. BBB permeability and KRG

Claudin-5 is tight junction protein in the BBB, and is associated with neurodegenerative disorders such as AD. Immunoblot analysis showed that Tg2576-Control group expressed lower level of Claudin-5 than that of WT group ($P < 0.01$). The expression of Claudin-5 was increased by KRG-administration ($P < 0.05$) (Fig. 4A). Immunohistochemistry (IHC) analysis also showed that KRG intake increased the expression of Claudin-5 (Fig. 4B).

Occludin, a protein for conjugation, showed lower expression in Tg2576-Control group than that of WT ($P < 0.01$). IHC showed that immuno-reactivity of Occludin was increased by KRG ingestion (Fig. 4B).

Laminin was also assessed, due to its role in regulating vascular integrity of the BBB. IHC analysis showed that Tg2576-Control group had lower Laminin expression compared to the WT group. In the Tg2576-ST 30 mg/kg/day group, Laminin expression was increased (Fig. 4C).

CD13 is the protein associated with the blood vessel formation, and it also showed that Tg2576-Control group had lower expression of CD13 than that of WT. However, it did not show significant change in the expression by KRG administration (Fig. 4C).

3.5. Changes in gut microbiota by KRG

Alteration of microbiota were observed by the 16S gene sequencing assay as for microbiota profiling method (Fig. 5). The genus diversity of Tg2576-Control is different from WT, showing less diversity when compared to WT (Fig. 5A, Fig. S1, S2). The difference in bacterial population distribution between WT and Tg2576-Control group was 0.024 (Q-vlaue <0.05). The species diversity showed the similar phenomenon (Fig. S3 - S5). KRG ingestion restored the diversity of the gut microbiota. In particular, Lactobacillus was increased during restoring process by ingestion of KRG.

LDA (Linear discriminant analysis) score confirmed that Lactobacillus colonies increased whereas those of Bifidobacterium, Ruminococcus, and Clostridia colonies decreased, with KRG at 30 mg/kg/day (Fig. 5B). With 100 mg/kg/day of KRG, Ruminococcus, Anaerostipes, and Clostridium colonies were decreased (Q-vlaue <0.05). The levels of Lactobacillus in the Tg2576-ST 30 mg/kg/day and 100 mg/kg/day groups were restored comparable to that of WT group.

3.6. Adverse events

During the two-week experimental period, there was no death or other adverse events by KRG administration. Increase in body weight curve in the control and in the administration group were within normal range (Fig. S6).

4. Discussion

In this study, we attempted to test the possibility between ginseng-induced cognitive enhancements through gut-brain axis concept. Using Tg2576 AD mice, we replicated the cognitive improvement by KRG intake. Biomarkers for BBB integrity were evaluated for the reason that BBB can be affected by AD, as well as the fact that BBB is the main selective barrier for the delivery molecules from blood to the brain, of which molecules being produced from gut microbiota changed by KRG. These experimental data support that KRG improves cognitive behavior and AD pathology by reducing Aβ aggregation and microglial activation with modulation of BBB integrity. Together with these results, we discovered Lactobacillus as the main microbiota affected by AD in the gut, which was restored by KRG.

It has not been reported that Lactobacillus may play a key role in AD pathology. Direct causal relationship between Lactobacillus and KRG-induced improvement in the brain needs to be determined, i.e. the potential role of gut brain axis. Gut-brain axis has been discovered as a new pathogenic or therapeutic target to approach neurobiological diseases since intestinal microbiota take part in bidirectional communication between the gut and the brain [19]. Intestinal microbiota influence neurodevelopment, modulate behavior, and contribute to neurological disorders [11]. The gut microbiota species differs in patients with AD, as one of the major

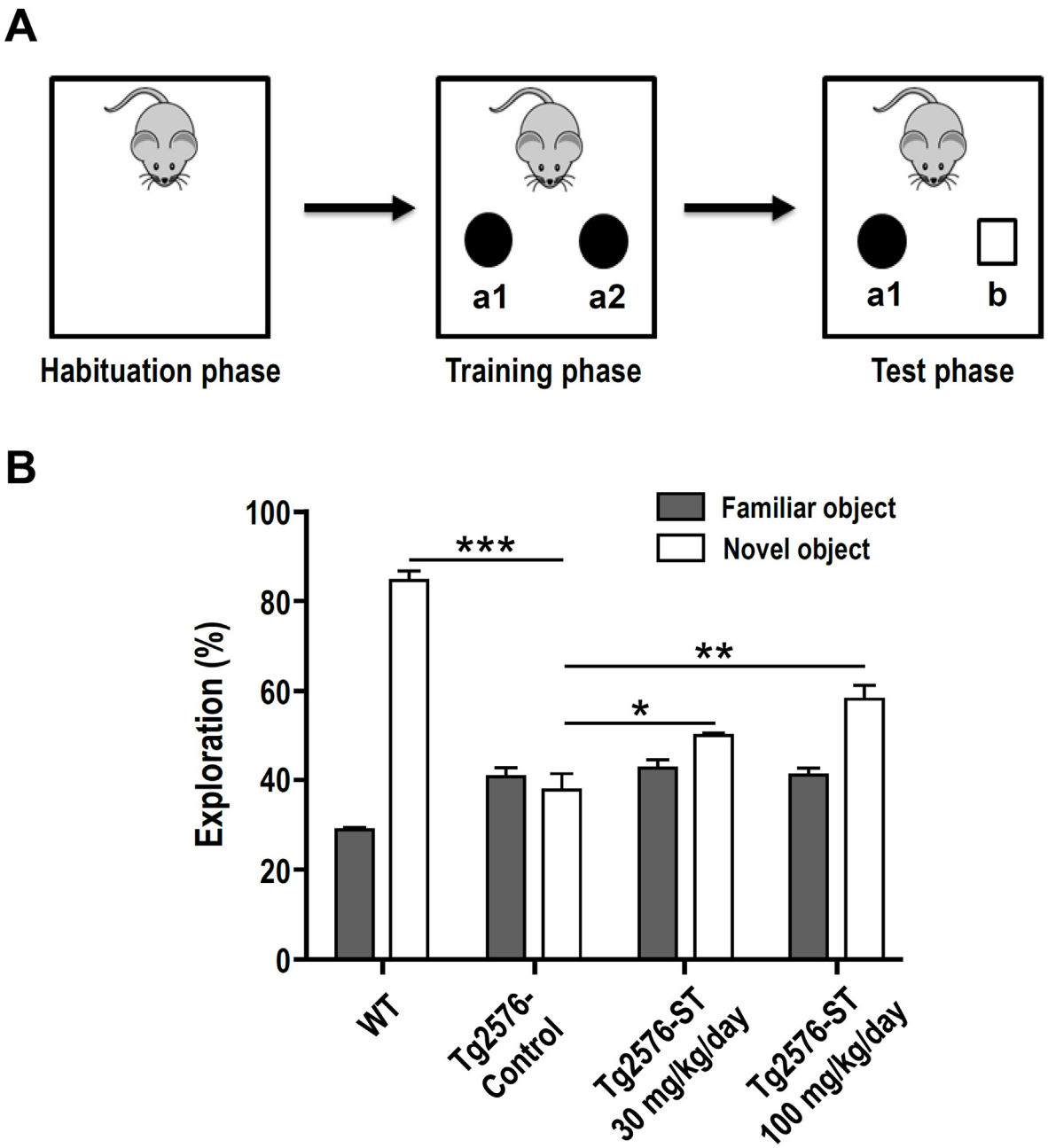

Fig. 1. Effects of KRG on novel object recognition test for mice of AD. (A) Scheme for Novel object recognition test. (B) The time spent by mouse for exploring the object zone. 14 days of KRG administration did not significantly affect the number of entries and time spent in the a2 area during the familiarization phase. Administration of KRG significantly reduced the number of entries and the time spent in the new object zone (b zone) during the testing phase. Compared with the WT group, Tg-2576 Control showed decreased number of novel objects. Compared to the Tg2576-Control group, KRG (30 and 100 mg/kg/day) treatment increased the number of novel objects. Results are expressed as the mean ± SD, n = 6, *P < 0.05, **P < 0.01, ***P < 0.001 compared to the Tg2576-Control group; *P < 0.05 compared to the Tg2576-ST 30 mg/kg/day group, and **P < 0.01 compared to the Tg2576-ST 100 mg/kg/day group.

risk factors that lead to progression of disease [35]. Accumulation of Aβ protein has been assumed to be the core pathological molecule in AD as it induces neurotoxicity through self-aggregation [6–10]. Therefore, previous findings and our result support that intestinal microbiota, especially Lactobacillus, can affect the pathology in the brain.

BBB permeability and the microglia activation is well-known pathologic phenomenon in AD. Thus, relationship between the changes in gut microbiota and the BBB permeability or the microglia activation [36–38] could support the modulation of AD through gut-brain axis. Microbiota can produce Aβ-like molecules resembling human CNS Aβ, that lead to protein misfolding and activation of microglia [39]. Therefore, controlling Aβ-like proteins generated in by intestinal microbiota can be another strategy [40]. Our results show plausible interaction between changes in microbiota and AD pathology through BBB integrity, such as Aβ protein accumulation and microglial activation [39]. From our experiment, KRG decreased the microglia activation and altered the BBB permeability. Claudin-5, Laminin, Occludin and CD13, were assessed for the BBB permeability [41] and the integrity of blood vessel [42]. Their different expression between Tg2576-Control and

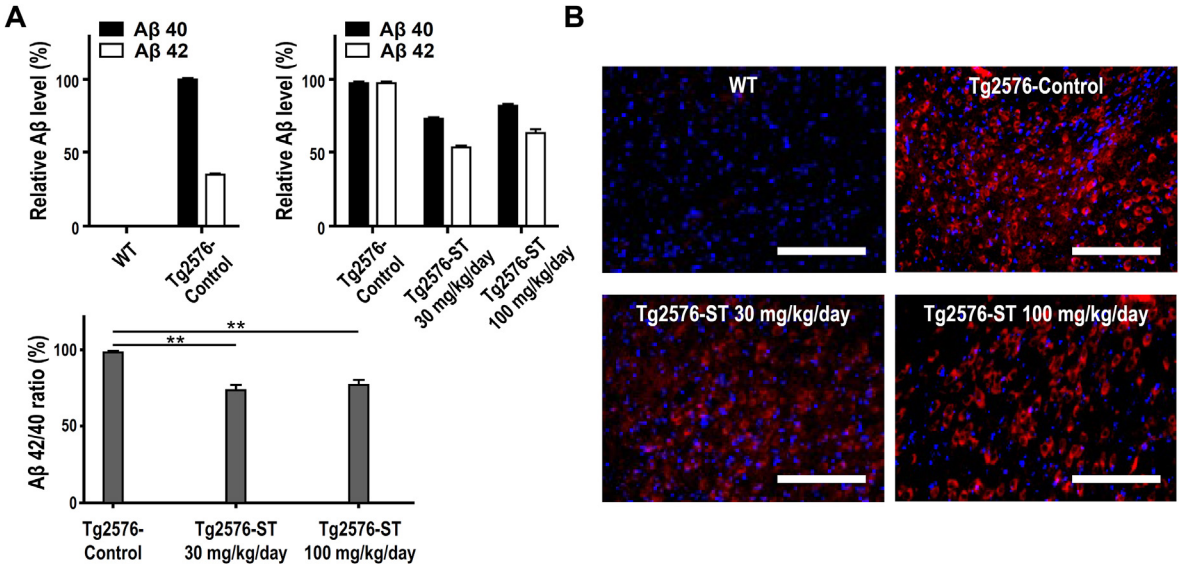

Fig. 2. Decreased insoluble Aβ oligomers by KRG treatment in the mice model of AD. (A) ELISA detection of soluble Aβ40, Aβ42, and Aβ42/Aβ40 ratio in each experimental groups. One-way ANOVA Turkey's post-hoc test was used to evaluate the statistical significance (*p < 0.05, **p < 0.01, ***p < 0.001). (B) Representative images stained with 6E10 (Red) antibody from hippocampal and cortical areas of each experimental groups. n = 6 mice per group. Scale bars represent 100 μm.

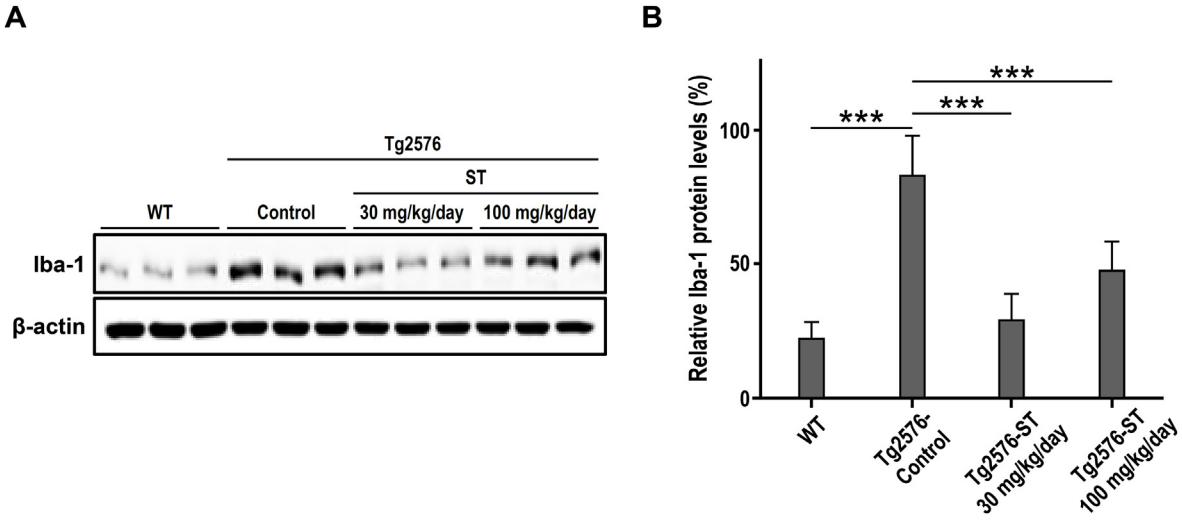

Fig. 3. Effect of KRG on the expression of Iba-1 in the mice model of AD. (A) Representative picture of Western blot for Iba-1 and β-actin. (B) Western blot for Iba-1 from the whole brain homogenates. The level of Iba-1 is expressed as mean ± SEM, which are normalized to β-actin in a same gel. One-way analysis of variance and the Tukey-Kramer multiple comparisons test were used to determine the statistically significant differences in the expression level of Iba-1 among the different groups. p < 0.001 for Tg2576-ST 30 mg/kg/day and, p < 0.001 for Tg2576-ST 100 mg/kg/day.

WT, and their improved integrity by KRG from our results support the previous findings.

Changes in microbiota by KRG can produce different metabolites, which might be related to AD pathology. Gut microbiota modulate microglia activation that causes neuronal damage with Aβ accumulation. A disruption in the gut microbiota can cause or progress AD through the gut-brain axis. Targeting the gut microbiota could be a promising approach in the amelioration of AD. In this study, we demonstrated that KRG ingestion modulates the AD pathology as well as change in the gut microbiota flora. These findings support the connection between the gut microbiota and AD through the gut-brain axis.

16S gene sequencing analysis confirmed that AD reduced the diversity of gut microbiota, in particular, it reduced the level of Lactobacillus. Following the administration of KRG for 14 days, the number of genes from microbial species became different, and the Lactobacillus was restored to the extent of WT group. Lactobacillus can affect the brain function by secreting acetyl choline into the blood stream, which plays role to memory and attention as a major neurotransmitter. Metabolites produced by the Lactobacillus are similar to those of human's, thus affect certain brain functions such as BBB permeability and microglial activation [21,41]. In addition, the effects of KRG is not enhanced at higher concentrations in most of results that are presented in this work. By the fact that anti-

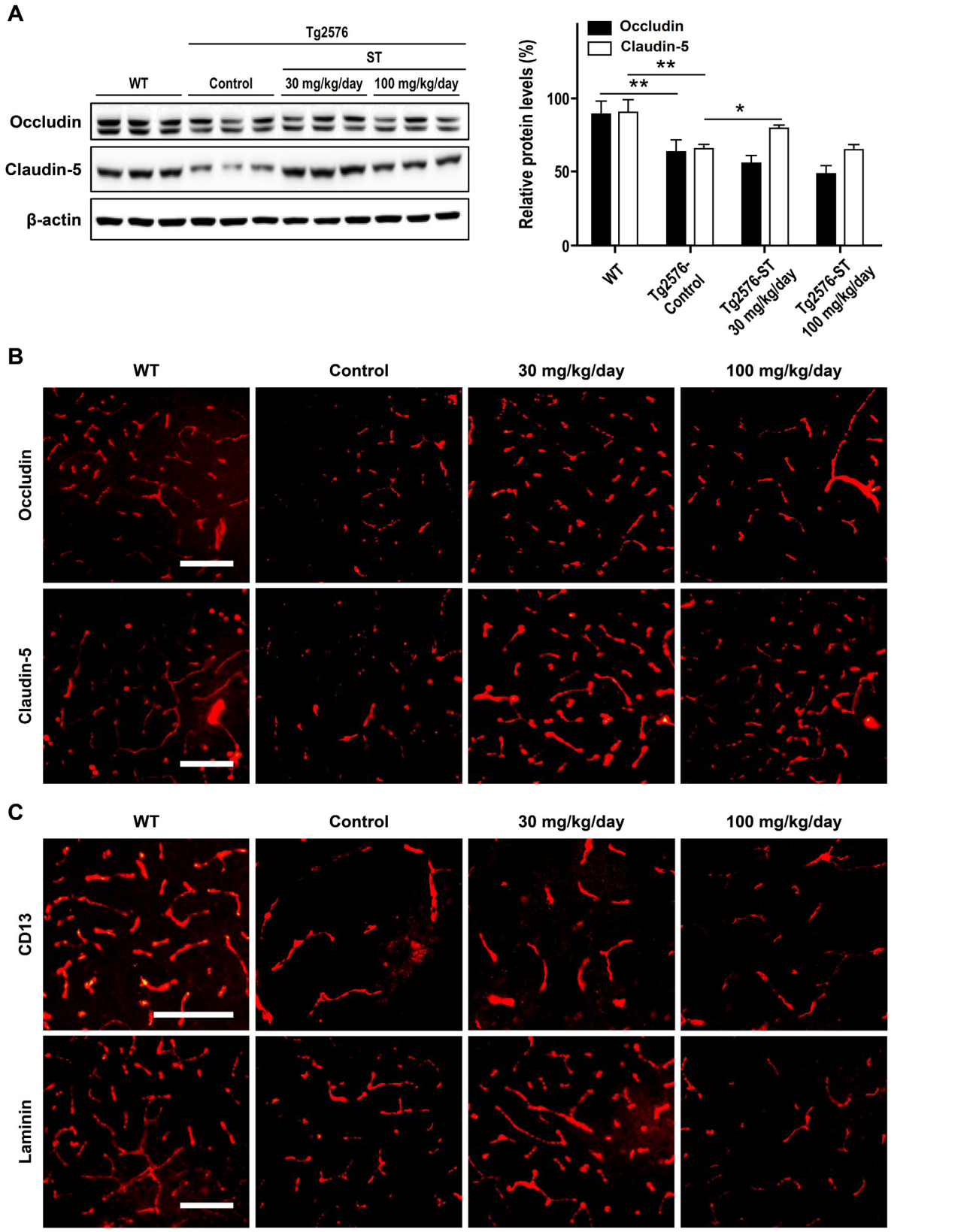

Fig. 4. Effect of KRG on the expression of endothelial Occludin, Claudin-5, Laminin and CD13 in the mice model of AD. (A) Immunoblots of protein extracts from brain parenchyma of mice from each experimental groups. The levels of Occludin and Claudin-5 were expressed as mean ± SEM, which are normalized to the level of β-actin in a same gel. One-way analysis of variance and the Tukey-Kramer multiple comparisons test were used to determine the statistically significant differences in the expression level of Claudin-5 among the different groups. *$p < 0.05$ for Tg2576-ST 30 mg/kg/day. In Tg2576-ST 30 mg/kg/day group, increased numbers of endothelial claudin-5 with morphological characteristics were observed compared to Tg2576-ST Control group. (B) Representative Images of tight junction proteins (Occludin, Claudin-5) in brain parenchyma in each experimental groups. (C) Representative Images of pericyte coverage of CD13 (red) in the cerebral cortex of mice in each experimental groups. Laminin (red) was used as an endothelial cell marker. Demonstrated data are the representative case from three experiments with six animals per condition per experiment, obtained from individual animals. (Scale bars: 100 μm).

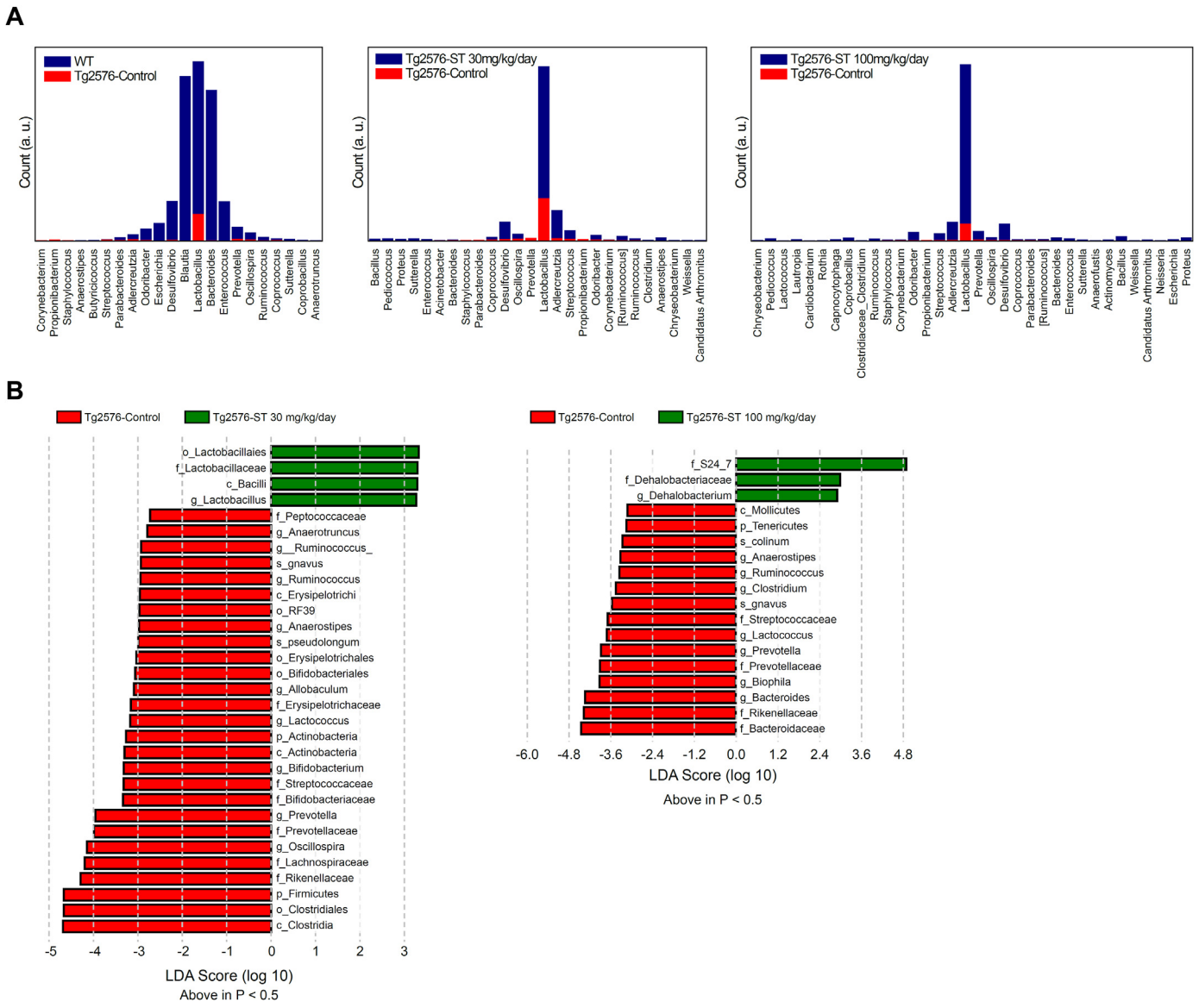

Fig. 5. Analysis of gut microbiota through 16S gene sequencing with fecal sample. (A) Representative genus levels of gut microbiota for WT, Tg2576-Control, Tg2576-ST 30 mg/kg/day, and Tg2576-ST 100 mg/kg/day. Lactobacillus levels in Tg-2576-ST 30 mg/kg/day and Tg2576-ST 100 mg/kg/day are significantly increased compared to that of Tg2576-Control. (B) LDA score for Tg2576-Control, Tg2576-ST 30 mg/kg/day, and Tg2576-ST 100 mg/kg/day (Q-value<0.05).

oxidation is one of the mechanisms by which KRG modulates AD, it can be inferred that above appropriate concentrations, excess KRG acted as oxidation source or performed side reactions which produce reactive radicals that could affect exacerbating the AD.

In summary, in the mice model of AD, KRG administration caused changes in the gut microbiota, especially the Lactobacillus. KRG administration also restored the BBB integrity and decreased microglial activation. Decreased microglia activation and BBB permeability change were associated with the reduction of Aβ accumulation and improvement in memory and cognition.

5. Conclusions

Here, we replicated the effect of KRG on improving the pathologies of AD in the mice model. It restored the reduced diversity of gut microbiota by AD, especially the level of Lactobacillus. BBB integrity, microglial activation, Aβ accumulation and cognitive behavior were monitored. Taken together, along with previous reported findings, KRG administration induced the Lactobacillus restoration, which can play a potential role through gut brain axis in Tg2576 AD mice.

Ethics approval and consent to participate

All experimental animal procedures performed were approved by the Institutional Animal Care and Use Committee (IACUC, Approval number: 16-0043-C2A1) of Seoul National University Hospital, which was accredited by the Association for the Assessment and Accreditation of Laboratory Animal Care International.

Consent for publication

All authors agreed to consent for publication.

Funding

This work was supported by 2019 grant from The Korean Society of Ginseng.

Authors' contributions

ML performed experiments, analyzed data, wrote paper, SL performed experiments, MK and KA performed the microbiome experiments, analysis, MK provided advice in study design, critically discussed results, co-edited paper. All authors have read and approved the manuscript.

Availability of data and materials

Data generated by and used in the study is available from the corresponding author upon reasonable request.

Declaration of competing interest

The authors declare that they have no competing interests.

Appendix A. Supplementary data

Supplementary data to this article can be found online at https://doi.org/10.1016/j.jgr.2021.11.001.

References

[1] Burns A, Iliffe S. Alzheimer's disease. BMJ 2009;338:b158.
[2] Li N, Liu Y, Li W, Zhou L, Li Q, Wang X, He P. A UPLC/MS-based metabolomics investigation of the protective effect of ginsenosides Rg1 and Rg2 in mice with Alzheimer's disease. J Ginseng Res. 2016;40:9–17.
[3] Zádori D, Veres G, Szalárdy L, Klivényi P, Vécsei L. Alzheimer's disease: recent concepts on the relation of mitochondrial disturbances, excitotoxicity, neuroinflammation, and Kynurenines. J Alzheimers Dis 2018;62:523–47.
[4] Association As. 2018 Alzheimer's disease facts and figures. Alzheimer's Dementia 2018;14:367–429.
[5] Hu Z, Wang L, Ma S, Kirisci L, Feng Z, Xue Y, Klunk WE, Kamboh MI, Sweet RA, Becker J, et al. Synergism of antihypertensives and cholinesterase inhibitors in Alzheimer's disease. Alzheimer's Dementia: Translational Research & Clinical Interventions 2018;4:542–55.
[6] Kwan KKL, Yun H, Dong TTX, Tsim KWK. Ginsenosides attenuate bioenergetics and morphology of mitochondria in cultured PC12 cells under the insult of amyloid beta-peptide. J Ginseng Res 2020;45:473–81.
[7] Bagyinszky E, Giau VV, Shim K, Suk K, An SSA, Kim S. Role of inflammatory molecules in the Alzheimer's disease progression and diagnosis. J Neurol Sci 2017;376:242–54.
[8] Hroudová J, Singh N, Fišar Z. Mitochondrial dysfunctions in neurodegenerative diseases: relevance to Alzheimer's disease. BioMed Res Int 2014;2014:175062.
[9] Manoharan S, Guillemin GJ, Abiramasundari RS, Essa MM, Akbar M, Akbar MD. The role of reactive oxygen species in the pathogenesis of Alzheimer's disease, Parkinson's disease, and Huntington's disease: a mini review. Oxidative Med Cell Longev 2016;2016:8590578.
[10] Zádori D, Veres G, Szalárdy L, Klivényi P, Toldi J, Vécsei L. Glutamatergic dysfunctioning in Alzheimer's disease and related therapeutic targets. J Alzheimers Dis 2014;42(Suppl 3):S177–87.
[11] Sampson TR, Debelius JW, Thron T, Janssen S, Shastri GG, Ilhan ZE, Challis C, Schretter CE, Rocha S, Gradinaru V, et al. Gut microbiota regulate motor deficits and neuroinflammation in a model of Parkinson's disease. Cell 2016;167:1469–80. e12.
[12] He Y, Kosciolek T, Tang J, Zhou Y, Li Z, Ma X, Zhu Q, Yuan N, Yuan L, Li C, et al. Gut microbiome and magnetic resonance spectroscopy study of subjects at ultra-high risk for psychosis may support the membrane hypothesis. Eur Psychiatr 2018;53:37–45.
[13] Gülden E, Chao C, Tai N, Pearson JA, Peng J, Majewska-Szczepanik M, Zhou Z, Wong FS, Wen L. TRIF deficiency protects non-obese diabetic mice from type 1 diabetes by modulating the gut microbiota and dendritic cells. J Autoimmun 2018;93:57–65.
[14] Li YY, Pearson JA, Chao C, Peng J, Zhang X, Zhou Z, Liu Y, Wong FS, Wen L. Nucleotide-binding oligomerization domain-containing protein 2 (Nod 2) modulates T1DM susceptibility by gut microbiota. J Autoimmun 2017;82:85–95.
[15] Li J, Zhao F, Wang Y, Chen J, Tao J, Tian G, Wu S, Liu W, Cui Q, Geng B, et al. Gut microbiota dysbiosis contributes to the development of hypertension. Microbiome 2017;5:14.
[16] Peng J, Xiao X, Hu M, Zhang X. Interaction between gut microbiome and cardiovascular disease. Life Sci 2018;214:153–7.
[17] Ye Z, Zhang N, Wu C, Zhang X, Wang Q, Huang X, Du L, Cao Q, Tang J, Zhou C, et al. A metagenomic study of the gut microbiome in Behcet's disease. Microbiome 2018;6:135.
[18] Jiang C, Li G, Huang P, Liu Z, Zhao B. The gut microbiota and Alzheimer's disease. J Alzheimers Dis 2017;58:1–15.
[19] Sochocka M, Donskow-Łysoniewska K, Diniz BS, Kurpas D, Brzozowska E, Leszek J. The gut microbiome alterations and inflammation-driven pathogenesis of Alzheimer's disease-a critical review. Mol Neurobiol 2019;56:1841–51.
[20] Braniste V, Al-Asmakh M, Kowal C, Anuar F, Abbaspour A, Tóth M, Korecka A, Bakocevic N, Ng LG, Kundu P, et al. The gut microbiota influences blood-brain barrier permeability in mice. Sci Transl Med 2014;6. 263ra158.
[21] Rybnikova E. Brain, antibiotics, and microbiota – how do they interplay? J Neurochem 2018;146:208–10.
[22] Kim J-H. Pharmacological and medical applications of Panax ginseng and ginsenosides: a review for use in cardiovascular diseases. J Ginseng Res 2018;42:264–9.
[23] Kim KH, Lee D, Lee HL, Kim C-E, Jung K, Kang KS. Beneficial effects of Panax ginseng for the treatment and prevention of neurodegenerative diseases: past findings and future directions. J Ginseng Res 2018;42:239–47.
[24] Fang F, Chen X, Huang T, Lue LF, Luddy JS, Yan SS. Multi-faced neuroprotective effects of Ginsenoside Rg1 in an Alzheimer mouse model. Biochim Biophys Acta 2012;1822:286–92.
[25] Xie X, Wang HT, Li CL, Gao XH, Ding JL, Zhao HH, Lu YL. Ginsenoside Rb1 protects PC12 cells against β-amyloid-induced cell injury. Mol Med Rep 2010;3:635–9.
[26] Wu J, Yang H, Zhao Q, Zhang X, Lou Y. Ginsenoside Rg1 exerts a protective effect against $A\beta_{25-35}$-induced toxicity in primary cultured rat cortical neurons through the NF-κB/NO pathway. Int J Mol Med 2016;37:781–8.
[27] Kim HJ, Jung SW, Kim SY, Cho IH, Kim HC, Rhim H, Kim M, Nah SY. Panax ginseng as an adjuvant treatment for Alzheimer's disease. J Ginseng Res. 2018;42:401–11.
[28] Wan Y, Wang J, J-f Xu, Tang F, Chen L, Tan Y-z, et al. Panax ginseng and its ginsenosides: potential candidates for the prevention and treatment of chemotherapy-induced side effects. J Ginseng Res 2021;45:617–30.
[29] Wang N, Wang X, He M, Zheng W, Qi D, Zhang Y. Han C-c. Ginseng polysaccharides: a potential neuroprotective agent. J Ginseng Res 2020;45:211–7.
[30] Im K, Kim J, Min H. Ginseng, the natural effectual antiviral: protective effects of Korean Red Ginseng against viral infection. J Ginseng Res 2016;40:309–14.
[31] Kim D, Kwon S, Jeon H, Ryu S, Ha KT, Kim S. Proteomic change by Korean Red Ginseng in the substantia nigra of a Parkinson's disease mouse model. J Ginseng Res. 2018;42:429–35.
[32] Caporaso JG, Kuczynski J, Stombaugh J, Bittinger K, Bushman FD, Costello EK, Fierer N, Peña AG, Goodrich JK, Gordon JI, et al. QIIME allows analysis of high-throughput community sequencing data. Nat Methods 2010;7:335–6.
[33] Dhariwal A, Chong J, Habib S, King IL, Agellon LB, Xia J. Microbiome Analyst: a web-based tool for comprehensive statistical, visual and meta-analysis of microbiome data. Nucleic Acids Res 2017;45. W180–w8.
[34] DeSantis TZ, Hugenholtz P, Larsen N, Rojas M, Brodie EL, Keller K, Huber T, Dalevi D, Hu P, Andersen GL. Greengenes, a chimera-checked 16S rRNA gene database and workbench compatible with ARB. Appl Environ Microbiol 2006;72:5069–72.
[35] Köhler CA, Maes M, Slyepchenko A, Berk M, Solmi M, Lanctôt KL, Carvalho AF. The gut-brain Axis, including the microbiome, leaky gut and bacterial translocation: mechanisms and pathophysiological role in Alzheimer's disease. Curr Pharmaceut Des 2016;22:6152–66.
[36] Abdel-Haq R, Schlachetzki JCM, Glass CK, Mazmanian SK. Microbiome–microglia connections via the gut–brain axis. J Exp Med 2018;216:41–59.
[37] Tang W, Zhu H, Feng Y, Guo R, Wan D. The impact of gut microbiota disorders on the blood-brain barrier. Infect Drug Resist 2020;13:3351–63.
[38] Zhu S, Jiang Y, Xu K, Cui M, Ye W, Zhao G, Jin L, Chen X. The progress of gut microbiome research related to brain disorders. J Neuroinflammation 2020;17:25.
[39] Bonfili L, Cecarini V, Gogoi O, Gong C, Cuccioloni M, Angeletti M, et al. Microbiota modulation as preventative and therapeutic approach in Alzheimer's disease. FEBS J 2020;288:2836–55 [n/a].
[40] Kowalski K, Mulak A. Brain-gut-microbiota Axis in Alzheimer's disease. J Neurogastroenterol Motil 2019;25:48–60.
[41] Braniste V, Al-Asmakh M, Kowal C, Anuar F, Abbaspour A, Tóth M, Korecka A, Bakocevic N, Ng LG, Kundu P, et al. The gut microbiota influences blood-brain barrier permeability in mice. Sci Transl Med 2014;6. 263ra158.
[42] Takeshita Y, Fujikawa S, Omoto M, Shimizu F, Maeda T, Sano Y, Kanda T. The effect of blood-brain barrier (BBB)-specific laminins for barrier function with a new in vitro BBB model incorporating multi-culturing system of BBB components. J Neurol Sci 2017;381:966.